CALCULATION OF SKY VIEW FACTOR AND ROUGHNESS PARAMETERS IN A MEDIUM SIZED CITY

T GÁL and J UNGER

Department of Climatology and Landscape Ecology, University of Szeged, POBox. 653, 6701 Szeged, Hungary
E-mail: tgal@geo.u-szeged.hu

Summary: Studying the altered urban environment is important because of the high number of the involved inhabitants. In urban areas surface cover and geometry differ from the rural surfaces, and the water and energy balances are modified. As a result the thermal environment and the airflow conditions are modified, and these modifications affect the energy consumption and wind energy potential in urban areas. The evaluation of the urban surface geometry and its parameters are not straightforward, and still a rapidly developing field of research. In this paper new software methods for the calculations of urban surface parameters are presented. These software tools enable us to evaluate the building and tree-crown databases from spectral and elevation data, and to use these two datasets to calculate SVF and roughness parameters. These software tools were applied for the study area in Debrecen, Hungary, in order to test the methods and to gather information about the variance of the urban surface in this city. Using the results the heating/cooling energy demand of the households and the wind energy potential can be estimated in urban areas.

Key words: building and tree datasets, mapping tools, surface geometry, urban climate

1. INTRODUCTION

Studying the altered urban environment is important because of the high number of the involved inhabitants. The surface cover and geometry differ from the rural surfaces, and the water and energy balances are modified (Oke 1987). Urban climate research focuses on this modified local climate. This is a priority topic since the prediction of the possible impacts of global climate change for urban areas is impossible without an in-depth knowledge of the features of urban climate. The two most important modifications of the climate in these areas are the altered thermal environment and the different airflow conditions, and both of these climate modifications are primarily connected with the alteration of the geometry and material characteristics of the surface (Oke 1987).

The thermal modification often appears in urban temperatures being higher than in the surrounding rural areas (urban heat island − UHI). The largest UHI, which is the strongest urban-rural temperature contrast, generally appears at night, while during the daytime the difference is moderate or absent. The main reason of the UHI is the urban-rural difference in the nocturnal cooling processes, which are primarily forced by outgoing long wave radiation. In urban areas the 3D geometrical configuration of the surface plays an important role in the restriction of long-wave radiative heat loss, and contributes to intra-urban temperature variations below roof level (Oke 1981). The sky view factor (SVF) is the most appropriate parameter describing the urban geometry (Oke 1981, Svensson 2004). SVF is defined as the

ratio of the radiation received (or emitted) by a planar surface and the radiation emitted (or received) by the entire hemispheric environment (Watson and Johnson 1987). It is a dimensionless measure between zero and one, representing totally obstructed and free spaces, respectively (Oke 1988). This parameter is also essential for the estimation of the solar potential in urban areas because the higher the SVF at a surface point the greater its openness to the sky thus the larger its solar potential too.

Due to the increased drag of the surface the average wind speed is lower in the cities than in the surrounding rural areas (Oke 1987). For describing the geometry or texture of the surface and as a consequence its roughness several parameters are known (Grimmond and Oke 1999). The connection between the wind and the drag force of the obstacles (buildings, vegetation) can be characterized by the zero-plane displacement height (z_d) and the aerodynamical roughness length (z_0) (Counihan 1971). These are the key parameters in studying the urban atmosphere, and at the same time these are the basic parameters for the estimation of intra-urban wind energy potential.

There are several options to calculate SVF values in urban environment (see Unger (2009) and Chen et al. (2012) for brief reviews). One way is the application of computer algorithms that requires a 3D surface database about the examined area. These methods can be separated by the input data used (raster or vector). Most of them utilize high resolution raster digital surface models containing the terrain and the buildings for computing patterns of continuous sky view factor (Lindberg 2007). Their advantage is that the roof of buildings can be managed more easily; however the accuracy of the results is significantly affected by the selection of the resolution of the input data (Gál et al. 2009). There are some examples for vector-based methods as well (Souza et al. 2003, Gál et al. 2009, Matzarakis and Matuschek 2010). These scripts calculate the SVF values more accurately because the buildings are in vector format, thus the locations of the building walls are unequivocal and do not depend on the resolution.

The determination of the roughness length (z_0) and displacement height (z_d) is not straightforward and remains problematic however there are numerous ways for their assessment or calculation. Three generalized classes of these methods are available: (1) micrometeorological methods using field observations of wind and turbulence, (2) roughness classification methods using roughness classes and visual estimation, (3) morphometric (or geometric) methods using measures of surface morphometry. The most common micrometeorological methods use data of field observations from one or a few installed and instrumented tall towers for the computation of z_0 and z_d based on the log-law (Grimmond and Oke 1999). The micrometeorological methods are unsuitable for detailed roughness mapping; however they are suitable for the validation of the other surface roughness calculation procedures. With the classification methods roughness can be estimated based on earlier measurements of the roughness values in a similar terrain elsewhere. The well-known Davenport method distinguishes eight roughness classes and it uses the eye as integrator of photographs or land use maps (Davenport et al. 2000). This method is based on the decisions of the researcher who evaluates the input data, thus it is not suitable for the development of a roughness calculation software. There are several morphometric methods using surface morphology data (Counihan 1971, Bottema 1997, Grimmond and Oke 1999). These methods are based on empirical relations from wind tunnel studies concerning flows over regular building arrangements and there are only a few examples of their generalization.

The roughness parameters are widely used for wind speed reduction in urban sites where in situ measurements are not available. Wind speed at 2 or 10 m above ground level is a key input parameter for microclimate modeling for example in ENVI-met (Lahme and Bruse 2003, Égerházi et al. 2013) or in the RayMan model (Matzarakis et al. 19), and it is also applied for the

calculation or modeling of human thermal comfort parameters (Spangolo and de Dear 2003, Kántor and Unger 2011, Bröde et al. 2012).

The aims of this study are (i) to present a new automatic software method for the calculation of sky view factor and roughness parameters, and (ii) to apply these methods in a medium sized city (Debrecen, Hungary).

2. STUDY AREA AND THE APPLIED DATABASE

The study area is located in Debrecen (47.5°N, 21.5°E). The city lies at a height of 120 m above sea level on nearly flat terrain in the Great Hungarian Plain, which is favorable for UHI development (Fig. 1). It is the second largest city in Hungary with a population of 220 000. Debrecen is the cultural, academic and economic centre of the northeastern region of the country.

The city's region belongs to the Köppen climate type Cfb on the basis of the 1961–90 climate normal, but it has a significant year-by-year fluctuation. The annual amount of precipitation is about 550 mm and its variation shows a maximum in May and June. Generally, the summer is sunny and warm, with an average temperature above 20 °C. The winter is cold; it is around -2 °C and it is often snowy. The wind speed is usually around 3 ms^{-1} and the prevailing wind direction is northeasterly (Bottyán et al. 2005).

The study area was divided to 1 km × 1 km grid and the roughness parameters were calculated for the center points of each grid (Fig. 1). The SVF varies at the local scale therefore it is not reasonable to present its intra-urban variation in the entire city area. So three grid cells representing the most important built-up types of the city were selected (Fig. 1): compact midrise, open midrise and open low-rise.
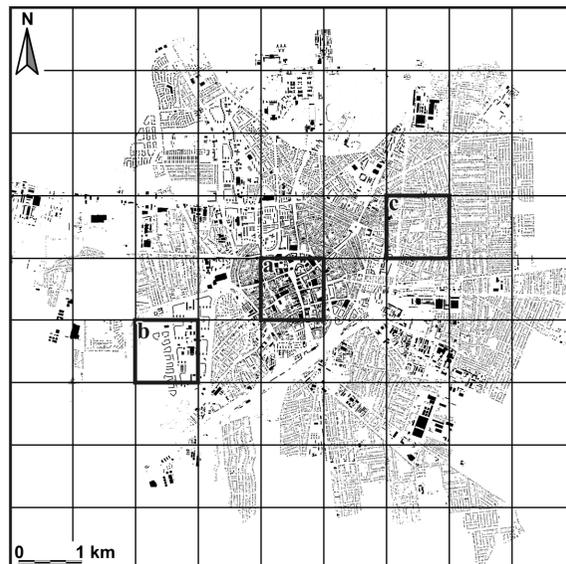

Fig. 1 Study area with the 1 km grid for roughness calculation and the areas
(a: compact midrise, b: open midrise, c: open low-rise) for SVF calculation

Detailed building and tree-crown databases were used as inputs for the SVF and roughness calculations in the study area. These databases were calculated with a tree-crown mapping tool (TCM) (Fábián 2012, Gál et al. 2013). This standalone automatic software tool was developed in C++ language and it is compatible with Windows and Linux environments.

The basic parameter for tree crown mapping was the Normalized Vegetation Index (NDVI). NDVI is calculated from the red and near infrared pixel values of the aerial image, it is between -1 and +1 and the values between 0.2 and 1 represent the areas where the amount vegetation (biomass) is high (Lillesand and Kiefer 1987). Elevation information was stored in comma-separated text files and the outputs of the software were in two shapefiles containing the building and tree crown databases (Gál et al. 2013). The NDVI represents the ratio of the vegetation thus it is important for deciding whether a point (a pixel in an aerial photograph) belongs to a building or to a tree. If the NDVI indicates that this point is a part of a tree crown, it is classified as tree crown, even if there is a building roof under it.

In this case the source of the elevation data was a 3D point cloud calculated by photogrammetric method. For the evaluation of the 3D point cloud and calculation of NDVI 4-band digital aerial photographs were used, taken by the Hungarian Institute of Geodesy, Cartography and Remote Sensing in 2007. The resolution of the photographs is approximately 0.5 m and they have 4 spectral bands (3 visible and 1 near infrared). Due to their spectral and spatial resolution these bands are suitable for calculating high resolution spectral indices (e.g. NDVI), also for applying photogrammetric methods for height measurements at the same time. This kind of aerial photographs are commonly used for cartographical issues, and they can be accessed easily in most of the countries (Gál and Unger 2012). The evaluation of the aerial photographs was carried out with the Leica Photogrammetry Suit, and for the height measurements its enhanced Automatic Terrain Extraction (eATE) tool was used.

As an optional input the TCM can use building footprints and tree-crown border lines in ESRI shape files. If these files are available the calculation time can be significantly shorter. In our case a building footprint database was applied as an input, which was calculated from the digital cadastral map of Debrecen.

The localization of the tree-crowns is based on the NDVI values. The shapes of the tree-crowns are calculated by using Thiessen (or Voronoi) polygons (Aurenhammer 1991) around the points in the 3D point cloud. Tree crown points are localized by the software. All points in the 3D point cloud were identified as tree points, if the NDVI value in the same location was higher than 0.35 and grass areas if it is between 0.15 and 0.35. These values are based on a test in selected aerial photographs. During the test we calculated the NDVI values for several typical tree crowns and for typical other vegetation patches (grass, etc). Also, the method selects tree points in a small area, where there are no other (non-tree) points inside the perimeter of this selection, and the difference of the elevation of the points is below a threshold (0.5 m in this case). Finally, a Voronoi polygon was plotted around of this set of tree points. Within all of these polygons two different elevation values are calculated: (i) tree top height (the average of the highest 5% of the measured elevations), (ii)
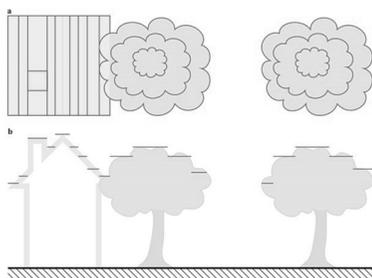

Fig. 2 Concept of the building and tree-crown databases (a: footprint, b: side view)

tree perimeter height (the average of the lowest 5% of the measured elevations). Hereinafter we use only this second elevation value.

The obtained building and tree-crown databases contain polygons (bordered by not only straight but curved lines too) representing the parts of the roofs or trees where the elevation values are approximately the same (Fig. 2). In our case the building database was calculated using the building footprints, thus we have only 2 height values for each building (roof top and eaves heights).

The building and tree-crown databases were evaluated for the whole study area. Fig. 3 illustrates a small part of it in the center of Debrecen.
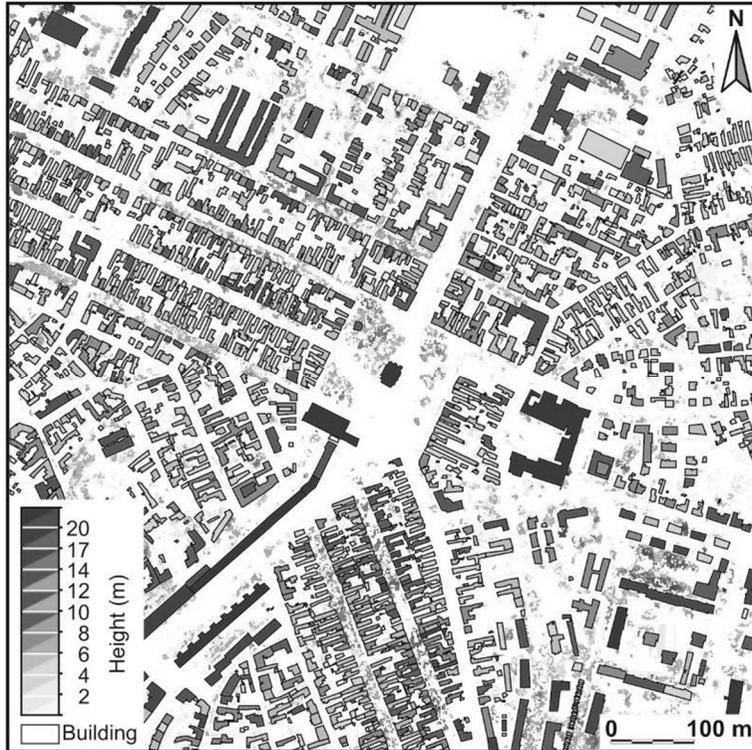

Fig. 3 Building and tree-crown databases in the center of the whole study area

3. NEW CALCULATION METHODS

3.1. SVF mapping tool

The calculation of the SVF is based on a modified form of the equation by Unger (2009) and Gál et al. (2009). It takes into account the effect of different object types on the SVF. These objects are: building (B) with the highest elevation angle (β) in a given direction from a given point, tree (T_1) with the highest elevation angle ($\beta + \gamma$) in the same direction, and tree (T_2) with the highest zenith angle (δ) of the crown overlapping the point where the SVF calculation was made (Fig. 4).
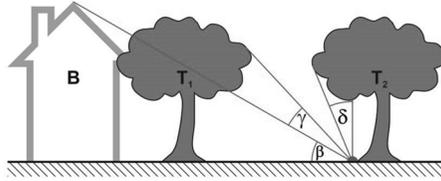
25

Fig. 4 Elevation angles for the different objects in a given direction

The value of the SVF for a given point is equal to one minus the sum of the view factors (VF) of different objects (B, T_1, T_2) in all directions (ω):

$$SVF = 1 - \left(\int_0^{2\pi} VF_B \, d\omega + \int_0^{2\pi} \tau \cdot VF_{T_1} d\omega + \int_0^{2\pi} \tau \cdot VF_{T_2} d\omega \right) \quad (1)$$

where τ is the transparency of the tree crowns. This transparency is considered to be constant and it describes the average transparency of the different tree species in the study area. In order to estimate the transparency we carried out field measurements and we obtained a τ value of 0.863591 (Gál and Unger 2012, 2014).

The calculations of the three different view factors were based on the equation for the calculations of SVF in a regular circle basin given by Oke (1987). For a regular basin, where β is the elevation angle from the centre to the wall, the SVF value (referring to the basin centre) is: $SVF_{basin} = \cos^2\beta$. So the view factor of a basin with the same elevation angle β is $VF_{basin} = 1 - \cos^2\beta = \sin^2\beta$. Therefore, if we have a regular circular building around the point of interest the view factor of this building is $VF_B = \sin^2\beta$. Similarly, the view factor of the first type trees is calculated using the angle γ with the following equation: $VF_{T1} = \sin^2(\beta + \gamma) - \sin^2\beta$ (Figs. 4 and 5). For the second type trees δ is used for calculation: $VF_{T2} = \sin^2 90° - \sin^2(90° - \delta) = 1 - \sin^2(90° - \delta)$.

In real situations the angular height of the objects is not equal in all directions; therefore the projection of the objects on the hemisphere is not a circle. In this case the three angular heights vary as a function of the direction (ω), so the Eq. 1 is modified:

$$SVF = 1 - \left(\int_0^{2\pi} \sin^2 \beta \, d\omega + \int_0^{2\pi} \tau \cdot \left(\sin^2(\beta + \gamma) - \sin^2 \gamma \right) d\omega + \int_0^{2\pi} \tau \cdot \left(1 - \sin^2(90° - \delta) \right) d\omega \right) \quad (2)$$

To develop a computer algorithm, the utilization of Eq. 2 is not appropriate therefore the SVF value of this equation is estimated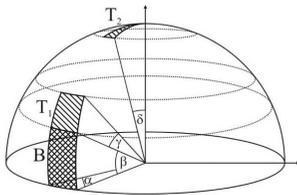 by using discrete sections of the hemisphere. The width of these sections is defined by the rotation angle α (Fig. 5) that determines the resolution of the calculation. If the value α decreases, i.e. the hemisphere is divided in small parts, the resolution and precision of the method increases since these describe the real layout of the objects around the point of interest more precisely.

Fig. 5 Polygons on the hemisphere corresponding to a building (B) and to the two types of tree-crowns (T_1 and T_2) (for explanation of angles see the text)

Using the angle α, Eq. 2 can be approximated with Eq. 3, where n is the number of divisions of the circle (n = 360°/α). In all directions only the elevation

angles (β, γ, δ) (Figs. 5 and 6) have to be determined for the calculation using the building and tree-crown databases.

$$SVF = 1 - \left(\sum_{i=1}^{n} \frac{\alpha}{2\pi} \cdot \sin^2 \beta_i + \sum_{i=1}^{n} \tau \cdot \frac{\alpha}{2\pi} \cdot \left(\sin^2 (\beta_i + \gamma_i) - \sin^2 \beta_i \right) + \sum_{i=1}^{n} \tau \cdot \frac{\alpha}{2\pi} \cdot \left(1 - \sin^2 (90° - \delta_i) \right) \right) \quad (3)$$

For the implementation of this calculation we developed a new software method in Java language. It is compatible with both Windows and Linux platforms, and it does not need any GIS software to operate (Gál and Unger 2014). This software reads the geometry and attributes information from the input building and tree crown shape files. For each SVF calculation point it scans the elements of the building and tree-crown databases with a projection line in a given (user defined) distance. The first direction of scanning line is North and then rotated clockwise by (user defined) angle α. The software calculates the highest elevation angles β and γ, and the largest zenith angles δ for all scanning lines; it also calculates the view factors for the different objects (B, T_1, T_2). The software applies a user defined constant transparency value (τ) during calculations. The calculation time is significantly low, the calculation of the SVF for one point takes only approximately 0.6 s in a common PC (Core i3 processor and 4 GB memory).

3.2. Roughness mapping tool

In our earlier research we have developed a new implementation for roughness calculation (Gál and Unger 2009). With this approach the calculation of the roughness parameters is possible not only for regular arrays of buildings and houses but also for irregular building groups as well as real urban sites (Gál and Unger 2009). The basis of the roughness length (z_0) computations is in accordance with the method of Bottema (1997). His basic model equation was originally designed for regular building groups:

$$z_0 = (h - z_d) \exp\left(- \frac{\kappa}{\sqrt{0.5 \cdot C_{Dh} \cdot \lambda_F}} \right) \quad (4)$$

where C_{Dh} is the drag coefficient for isolated obstacles and it is considered constant (0.8) (Bottema 1997), and λ_F is the frontal area ratio of an elementary area. The formula of the zero displacement height (z_d), which is necessary for Eq. 4, is a simple power-law approximation of the regular-group-model: $z_d = h \cdot (\lambda_P)^{0.6}$, where λ_P is the plan area ratio of an elementary area. In the case of irregular arrangements it gives an approximate value for z_d without taking the volume of the buildings and their recirculation zones into account.

The basis of the calculation of the input parameters is the building block; therefore the buildings touching each other were merged into blocks. As a next step we divided the study area into polygon-shape areas based on these blocks, which is a kind of extension of the approach used by Grimmond and Oke (1999). Each polygon consists of the set of points closer to the central building block than to the other blocks.

We defined the total surface area or lot area (A_T) as the area of a polygon. The sum of the areas of building footprints is the plan area for buildings (A_{Pb}). For the tree-crown parts in each polygon we have done the same in order to obtain the plan area for trees (A_{Pt}). The wind flow blocking attributed to the tree-crowns can be described using the porosity (p), which is a simple ratio of the perforated area to the total area of an obstacle (Heisler and DeWalle 1988). This p value for buildings is 0 but for deciduous trees it is characteristically

0.2 in winter and or 0.6 in summer owing to the variation of leaf cover. Using the porosity values the plan area ratio (λ_P) referred to a polygon is:

$$\lambda_P = (A_{Pb} + (1-p) \cdot A_{Pt}) / A_T \tag{5}$$

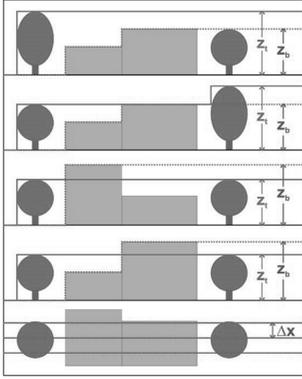In order to determine the frontal area ratio (λ_F) we have to compute the frontal area of

each building and tree-crown (Fig. 6). The frontal areas of buildings and trees depend on the direction of the airflow. The basis of the calculation is the frontal projection of the buildings and the tree-crowns within a lot polygon. This frontal projection could be calculated using projection lines with a given resolution (Δx). For each lines two height values are obtained: z_t for trees and z_b for buildings (Fig. 6). The frontal area for buildings (A_{Fb}) is the sum of the $\Delta x \cdot z_b$ values in each projection lines. The calculation of the frontal area of tree-crowns (A_{Ft}) is similar (sum of $\Delta x \cdot z_t$) if the value of z_t is higher than the value of z_b. In the case when the projection of a building is higher, the tree-crown is omitted from the calculation, because it has insignificant effect for the airflow compared to the building. The frontal area ratio referred to a polygon (and to an orientation) is:

Fig. 6 Concept of the frontal area calculation in a few different cases (for explanation of symbols see the text)

$$\lambda_F = (A_{Fb} + (1-p) \cdot A_{Ft}) / A_T \tag{6}$$

The calculation of the volumetrically averaged building height needs the volumes (V_{b1}, V_{b2}, V_{b3}, …, V_{bn}) and heights (h_{b1}, h_{b2}, h_{b3}, …, h_{bn}) of each building and also of tree-crowns (V_{t1}, V_{t2}, V_{t3}, …, V_{tn} and h_{t1}, h_{t2}, h_{t3}, …, h_{tn}) in each building block:
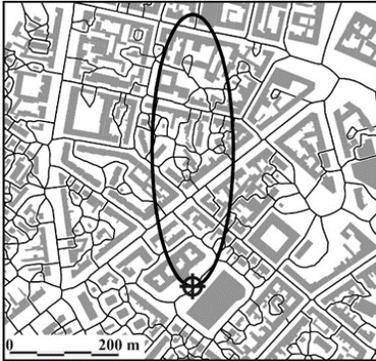

$$h = \frac{\sum_{i=1}^{n} V_{bi} \cdot h_{bi} + \sum_{j=1}^{n} \left(V_{tj} \cdot (1-p)\right) \cdot h_{tj}}{\sum_{i=1}^{n} V_{bi} + \sum_{j=1}^{n} \left(V_{tj} \cdot (1-p)\right)} \tag{7}$$

The final step is to take into account the effect of the surrounding areas. For this purpose we applied the concept of fetch (Liu et al. 2009). With this concept the effect of the source area (Schmidt 1994) for the airflow can be included into the calculation of the roughness parameters. In their work (Liu et al. 2009) the roughness length was calculated with four different morphometric methods in an elliptical area. The major and minor axis of these fetch were 500 and 150 m, respectively. The major axis was parallel to the wind direction, and the near endpoint of the windward placed fetch was at the measurement site (Fig. 7).

Fig. 7 Illustration of the fetch in an urban area (the cross shows the measurement site)

In our new method we use the similar approach. The roughness calculation refers to a point grid with an arbitrary resolution. For each point the roughness parameters are calculated with the following formulas:

$$z_0 = \frac{\sum\limits_{i=1}^{n} z_{0i} \cdot A_i}{\sum\limits_{i=1}^{n} A_i} \quad , \quad z_d = \frac{\sum\limits_{i=1}^{n} z_{di} \cdot A_i}{\sum\limits_{i=1}^{n} A_i} \tag{6}$$

where A_i is the overlapping area, z_{0i} is the roughness length, z_{di} is the displacement height of each lot polygon from the group of the polygons overlapping with the fetch (Fig. 7).

4. RESULTS

4.1. Intra-urban SVF patterns

The main characteristics of the spatial patterns of the calculated SVF values in the three different urban areas are significantly different. In the compact midrise area (Fig. 8a) the dominant range of SVF is 0.1–0.5, and only a few wide streets and urban squares have higher values. The dominance of the low SVF indicates that the long wave emission of the surface is mostly blocked in the urban canopy layer, thus at nighttime the cooling rate is moderate compared to the rural area.
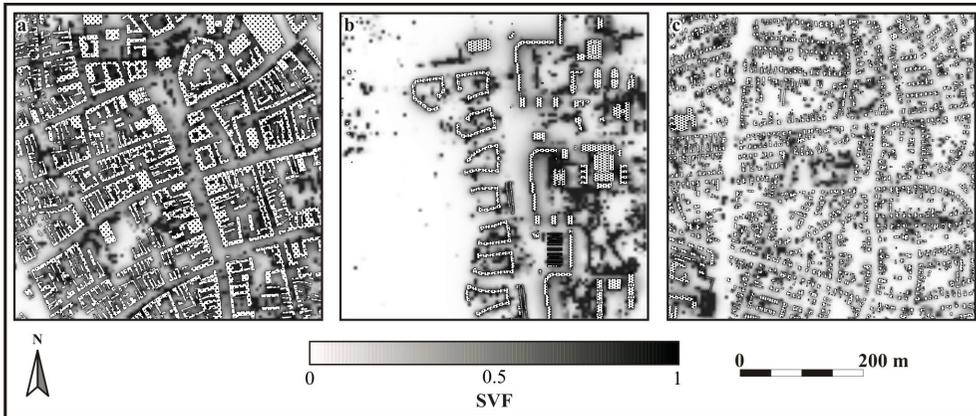

Fig. 8 Spatial patterns of the SVF in the three different urban areas
(a: compact midrise, b: open midrise, c: open low-rise)

In the open midrise area (Fig. 8b) the buildings are not smaller than in the compact midrise area, but the dominant range of the SVF decreased significantly. The values around 0.1–0.5 appear only in the close proximity of the buildings or in the urban parks with significant tree cover. In most of the streets the typical values are around 0.5–0.7. This difference indicates that the radiation balance and thermal reactions of this area are not so different from the rural ones like in the case of the compact midrise area.

In the open low-rise area (Fig. 8c) the typical SVF values are around 0.4–0.7, only some parts – with significant tree crown cover – have 0.1–0.3 values. The streets have 0.5–0.8 values and most of the backyards have the same or higher SVF because in these areas mostly low vegetation is present. These SVF values indicate that this kind of urban area has the least modified thermal properties and radiation balance within the presented types.

With the help of the obtained results of SVF calculation the thermal characteristics of the different built-up types can be identified. The compact midrise areas (city core) possibly have lower cooling rates at nighttime, thus the energy consumption of the households decreases in winter and increases in summer. This difference is less characteristic in the open midrise areas (housing estates) and the open low-rise (houses with gardens) areas. These results may help to calculate the energy consumption of these building types, which is essential for planning the necessary production by the renewable energy sources.

4.2. Roughness parameters in the study area

In the urbanized area of Debrecen the two most important roughness parameters show an almost concentric shape (Fig. 9). The zero displacement height (Fig. 9a) increases at the edge of the urban area and in the mostly open low-rise areas of the city it is around 2–5 m. At the edge of the inner city there is a rapid increase and in the city core its value reaches 12 m.

Roughness length increases rapidly in the edge of the city (Fig. 9b), the highest z_0 values appear in the center and in the open midrise areas (thanks to the 10-story buildings). In the center it reaches 2.5 m and in most of the city core it is larger than 1.5 m.
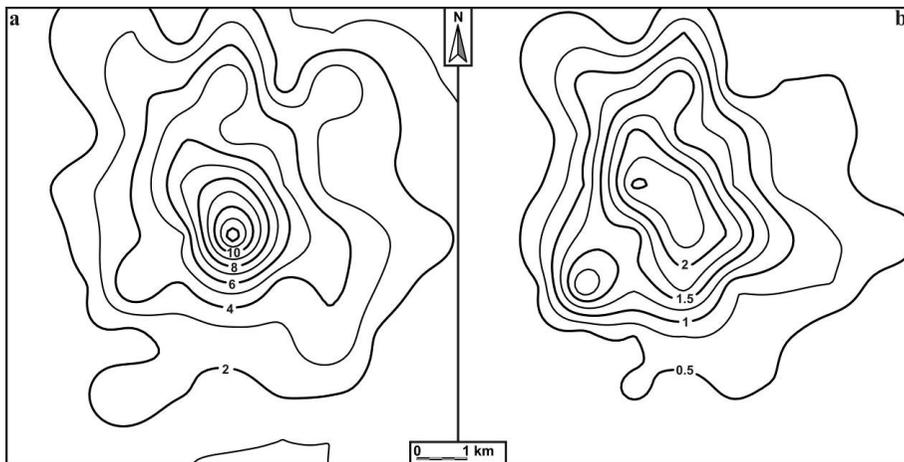

Fig. 9 Spatial distribution of displacement height (a) and roughness length (b) in m

Using these spatial patterns of the roughness parameters the most suitable areas for the development of the household-scale small wind turbines are mostly the open low-rise areas in the suburbs owing to the small enough z_0 and z_d values here. The tops of the high buildings in the open midrise areas may be also considered in this respect because of the relatively small roughness parameters. However, the city core is not appropriate for this purpose, namely the roughness parameters indicate high drag and decreased wind speed near the top of the buildings.

4. CONCLUSIONS

We presented new software methods for the calculation of urban surface parameters. These software tools enable us to evaluate the building and tree-crown database from spectral and elevation data, and using these two datasets to calculate SVF and roughness parameters. In this study we applied these software tools for a study area in Debrecen, Hungary, in order to test the methods and to gather information about the variance of the urban surface in this city. Using the results of this study the heating/cooling energy demand of the households and the wind energy potential can be estimated in urban areas.

REFERENCES

Aurenhammer F (1991) Voronoi diagrams – A survey of fundamental geometric data structure. ACM Comput Surv 23:345-405

Bottema M (1997) Urban roughness modelling in relation to pollutant dispersion. Atmos Environ 31:3059-3075

Bottyán Z, Kircsi A, Szegedi S, Unger J (2005) The relationship between built-up areas and the spatial development of the mean maximum urban heat island in Debrecen, Hungary. Int J Climatol 25:405-418

Bröde P, Fiala D, Błażejczyk K, Holmér I, Jendritzky G, Kampmann B, Tinz B, Havenith G (2012) Deriving the operational procedure for the Universal Thermal Climate Index (UTCI). Int J Biometeorol 56:481-494

Chen L, Ng E, An X, Ren C, Lee M, Wang U, He Z (2012) Sky view factor analysis of street canyons and its implications for daytime intra-urban air temperature differentials in high-rise, high-density urban areas of Hong Kong: a GIS-based simulation approach. Int J Climatol 32:121-136

Counihan J (1971) Wind tunnel determination of the roughness length as a function of fetch and density of three-dimensional roughness elements. Atmos Environ 5:637-642

Davenport AG, Grimmond CSB, Oke TR, Wieringa J (2000) Estimating the roughness of cities and sheltered country. In: Proc 12th Conf Appl Climatol, Boston, USA. 96-99

Égerházi LA, Kovács A, Unger J (2013) Application of microclimate modelling and onsite survey in planning practice related to an urban micro-environment. Adv Meteorol 251586

Fábian PÁ (2012) Derivation of tree-crown database using spectral and height information in an urban area (in Hungarian). MSc Thesis, University of Szeged, Szeged, Hungary

Gál T, Unger J (2009) Detection of ventilation paths using high-resolution roughness parameter mapping in a large urban area. Build Environ 44:198-206

Gál T, Unger J (2012) Surface geometry mapping for SVF calculation in urban areas. In: Proc 8th Int Conf on Urban Climate and 10th Symp on Urban Environ, Dublin, Ireland. Paper 168

Gál T, Unger J (2014) A new software tool for SVF calculations using building and tree-crown databases. Urban Clim 10:594-606

Gál T, Lindberg F, Unger J (2009) Computing continuous sky view factor using 3D urban raster and vector databases: comparison and an application for urban climate. Theor Appl Climatol 95:111-123

Gál T, Unger J, Kiss M (2013) An automatic method to create an urban vegetation database using 4 band aerial photographs for Sky View Factor calculation – A case study in Szeged, Hungary. In: Proc. Two hundred years of urban meteorology in the heart of Florence: Int Conf on Urban Climate and History of Meteorol, Florence, Italy. 124-132

Grimmond CSB, Oke TR (1999) Aerodynamic properties of urban areas derived from analysis of surface form. J Appl Meteorol 34:1262-1292

Heisler GM, DeWalle DR (1988) Effect of wind break structure on wind flow. Agr Ecosyst Environ 22-23:41-69

Kántor N, Unger J (2011) The most problematic variable in the course of human-biometeorological comfort assessment – the mean radiant temperature. Cent Eur J Geosci 3:90-100

Lahme E, Bruse M (2003) Microclimatic effects of a small urban park in densely built-up areas: Measurements and model simulations. In: Proc. 5th Int Conf on Urban Climate, Lodz, Poland. P.5.1

Lillesand TM, Kiefer RW (1987) Remote sensing and image interpretation. J. Wiley and Sons, Hoboken

Lindberg F (2007) Modelling the urban climate using a local governmental geo-database. Meteorol Appl 14:263-273

Liu G, Sun J, Jiang W (2009) Observational verification of urban surface roughness parameters derived from morphological models. Meteorol Appl 16:205-213

Matzarakis A, Matuschek O (2010) Sky View Factor as a parameter in applied climatology – Rapid estimation by the SkyHelios Model. Meteorol Z 20:39-45

Matzarakis A, Rutz F, Mayer H (2007) Modelling radiation fluxes in simple and complex environments - application of the RayMan model. Int J Biometeorol 51:323-334

Oke TR (1981) Canyon geometry and the nocturnal urban heat island: comparison of scale model and field observations. J Climatol 1:237-254

Oke TR (1987) Boundary layer climates. Routledge, London-New York

Oke TR (1988) Street design and urban canopy layer climate. Energ Buildings 11:103-113

Schmid HP (1994) Source areas for scalars and scalar fluxes, Bound-Lay Meteorol 67:293-318

Souza LCL, Rodrigues DS, Mendes JFG (2003) The 3DSkyView extension: an urban geometry acces tool in a geographical information system. In: Proc 5th Int Conf on Urban Climate, Lodz, Poland. O.31.3

Spagnolo JC, de Dear RJ (2003) A human thermal climatology of subtropical Sydney. Int J Climatol 23:1383-1395

Stewart ID, Oke TR (2012) Local Climate Zones for urban temperature studies. B Am Meteorol Soc 93:1879-1900

Svensson M (2004) Sky view factor analysis – implications for urban air temperature differences. Meteorol Appl 11:201-211

Unger J (2009) Connection between urban heat island and sky view factor approximated by a software tool on a 3D urban database. Int J Environ Pollut 36:59-80

Watson ID, Johnson GT (1987) Graphical estimation of sky view-factors in urban environments. J Climatol 7:193-197